Title

MEASUREMENT OF VIBRATION-ROTATION LINE STRENGTHS OF HO USING A TUNABLE DIODE LASER

Authors

Podolske, J.R.
Johnston, H.S.

Publication Date

1983-06-01

LBL-16370
Preprint

Lawrence Berkeley Laboratory
UNIVERSITY OF CALIFORNIA

Materials & Molecular Research Division

Submitted to the Journal of Chemical Physics

MEASUREMENT OF VIBRATION-ROTATION LINE STRENGTHS OF HO USING A TUNABLE DIODE LASER

J.R. Podolske and H.S. Johnston

June 1983

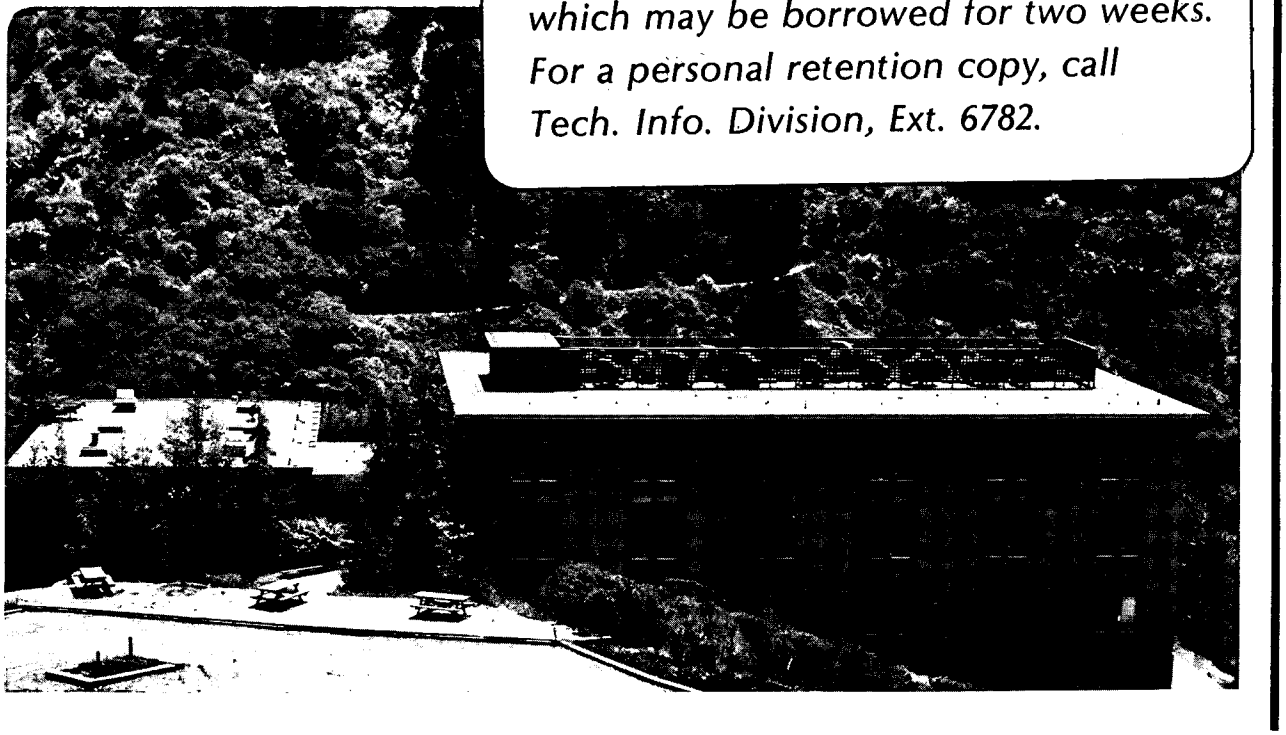

Prepared for the U.S. Department of Energy under Contract DE-AC03-76SF00098

DISCLAIMER

Measurement of Vibration-Rotation Line Strengths of HO Using a Tunable Diode Laser

By

James R. Podolske and Harold S. Johnston

Department of Chemistry and Materials and Molecular Research Division,

Lawrence Berkeley Laboratory, University of California,

Berkeley, California 94720

This work was supported by the Director, Office of Energy Research, Office of Basic Energy Sciences, Chemical Sciences Division of the U.S. Department of Energy under Contract Number DE-AC03-76SF00098.

ABSTRACT

Line strengths were measured for four transitions of the HO radical near 2.93 μm in the fundamental vibration-rotation band using a tunable infrared diode laser coupled to a molecular modulation spectrometer. The hydroxyl radical was produced by modulated photolysis of O_3 at 2537 Å in the presence of H_2O, and its number density obtained from numerical simulation of the complete photochemical system. The strongest line observed was at 3407.607 cm^{-1} with a measured line strength of $3.3 \pm 1.5 \times 10^{-20}$ cm^2 $molecule^{-1}$ cm^{-1}.

INTRODUCTION

The spectroscopy of the hydroxyl radical has been studied extensively over the last several decades because of its critical role in many diverse chemical systems including interstellar space,[1,2] the earth's atmosphere,[3,4] and combustion environments.[5] The first spectroscopic studies of HO were done on the $A^2\Sigma \leftarrow X^2\pi$ system in the 2800 - 3200 Å region, because of its high absorption and emission intensities and the convenient wavelength range. This band system has been utilized extensively both in absorption and emission to probe HO concentration in a variety of environments, and several analyses of this system have been done.[6-9] Recent work by Goldman and Gillis[9] gives line positions and intensities for this band at temperatures relevant to stratospheric and combustion studies (240 K and 4600 K, respectively). Results of studies in this region have been used in determining spectroscopic constants for the $X^2\pi$ electronic state.

The discovery by Meinel[10,11] of infrared vibration-rotation emission from vibrationally excited HO originating in the upper mesosphere and lower thermosphere from the exothermic reaction

$$H + O_3 \rightarrow OH\ (v \leq 9) + O_2 \qquad (1)$$

produced more spectroscopic information about the $^2\pi$ ground electronic state of HO and increased interest in the role of this radical in upper atmospheric photochemistry. Since then high resolution emission spectra of HO from intense sources were observed, and accurate line position data for transitions in the 0.9 - 3.7 nm region obtained.[12] These data were combined with line position data from $A^2\Sigma \leftarrow X^2\pi$ band studies and

microwave data on Λ splittings of low J $X^2\pi_i$ levels to produce good molecular constants and term values for the $X^2\pi_i$ state for $v \leq 5$.[13]

Although transition frequencies for the fundamental vibration band are known accurately from experiment and theory, line intensity information has been restricted to results of theoretical calculations[14] and inference from emission studies.[15] No direct measurement has been made due to the difficulty of preparing large radical concentrations, the relatively weak oscillator strength of these transitions and, previously, the lack of a suitable narrow-linewidth tunable spectral source. In this study a tunable diode laser was coupled to a molecular modulation spectrometer to measure the integrated absorption of four vibration-rotation transitions of HO, which was produced by the modulated photolysis of an O_3/H_2O mixture. Line strengths were determined from these measurements by calculating the component of the HO concentration which was observed during the modulated absorption measurement. These results now provide a method for measuring absolute HO concentrations.

EXPERIMENTAL

Moecular Modulation Spectrometer System

The experimental apparatus used for this study has been described previously.[22] It consists of a quartz-walled multipass absorption cell in a White configuration,[16] which serves as a photochemical reactor, and a combination UV and diode laser IR spectroscopic detection system. Several features of the apparatus which were illustrated but not described in reference 22 require some explanation.

The diode laser detection system can be operated in several modes. To make direct absorption measurements, the laser frequency is scanned slowly ($\sim$ 0.01 - 0.1 cm^{-1} min^{-1}) over a selected region by ramping the diode current, using the internal ramp generator of the Laser Control Module (LCM). The IR detector signal is carrier demodulated and sent to an x-y recorder whose x axis is driven by the ramp function of the LCM. This produces a direct record of the absorption spectrum of the reaction cell contents. To detect small absorptions (< 10%), first or second derivative detection works best.[17] A modulation ($\Delta\nu$) of the laser frequency is produced by feeding a 5 kHz sinewave to the LCM input, with $\Delta\nu$ set to be about 1/2 a typical absorption linewidth. The laser's center frequency is slowly scanned as before by the RCM ramp. Demodulation of the detector signal at the modulation frequency (5 kHz) or at twice the frequency (10 kHz) produces a signal approximately proportional to the first or second derivatives of the absorption line.[18] These signals can be recorded on the x-y recorder. This technique has high sensitivity and is good for determining line positions, but is difficult to calibrate for absolute absorption measurements.

The molecular modulation technique[19] was employed to investigate HO because it provides both the sensitivity of the derivative method and the quantitative results of direct absorption measurements. In this scheme, the HO radical concentration is modulated about a steady state value by sinusoidally modulating the photolytic lamp intensity about a D.C. level with an amplitude comparable to the average intensity. The flashing frequency chosen is usually a compromise between chemical modulation amplitude, which decreases with flashing frequency, and

signal-to-noise ratio of the IR detector and electronics, which increases with flashing frequency, and is typically between 0.5 - 50 Hz. The laser beam is chopped at a carrier frequency of 1800 Hz, passes through the cell, where it is further modulated by the varying absorber concentration, and finally is converted to an electrical signal by the IR detector. This signal is amplified and demodulated at the chopper frequency to produce a D.C. baseline component, I_o, which is recorded on the x-y recorder, and an A.C. component, ΔI, due to the chemical modulation, which is detected by a dual channel lock-in amplifier referenced to the photolytic lamps. The quantity ΔI is the vector sum of the measured in-phase ($A \cos \phi$) and quadrature ($A \sin \phi$) components of the signal

$$\Delta I = (A^2 \sin^2 \phi + A^2 \cos^2 \phi)^{1/2} \tag{2}$$

These observed quantities are related to the HO modulation amplitude (Δn) for small absorbances by

$$\Delta I / I_o = e^{-\sigma(\nu) \Delta n \ell} \tag{3}$$

where $\sigma(\nu)$ is the HO absorption cross section at the laser frequency ν and ℓ is the absorption pathlength. Since ℓ is known and Δn can be calculated (section IIc), $\sigma(\nu)$ can be measured directly. Scanning the laser over an entire HO absorption line then provides all the information needed to calculate its line strength

$$S = \int_{-\infty}^{\infty} \sigma(\nu) d\nu \tag{4}$$

In addition, the phase angle ϕ between the photolytic lamps and the HO modulation signal provides information about the HO lifetime in the photochemical system.

IR Absorption Measurements

The frequency and designation for each of the four HO transitions investigated are listed in Table I, along with frequencies for the H_2O reference lines. The HO transitions are also indicated on an energy level, Figure 1, which gives both the parity and e/f designation[20] for each state. Nuclear hyperfine splitting has been omitted for clarity. The intensity of the P(4.5) 1- line was measured absolutely by varying the chemical modulation frequency, and the intensities of the other three lines measured relative to it.

Run sequence 1 investigated the P(4.5) 1± lines near 3407.8 cm^{-1}. The monochromator was adjusted to span the expected position of these lines by using the 3407.826 cm^{-1} H_2O line as an absolute frequency reference and the etalon to measure frequency relative to the H_2O line. This H_2O line was observed by first derivative detection, as it is too weak to observe directly. The chemical conditions were then set to produce HO radical, with the photolysis lamps flashing at 15.6 Hz. Diode current was scanned over a 30 ma region at 1×10^{-4} A/s while I_o, A cos ϕ, and A sin ϕ were recorded. The resulting modulation amplitude signal is shown in Figure 2, along with frequency calibration traces. Peaks A and B come up exactly at the frequencies predicted for the P(4.5) 1- and P(4.5) 1+ lines, indicating that they are hydroxyl radical signals. A second scan of a 3 ma region near peak A was made at 1×10^{-5} A/s; the resulting modulation phase and amplitude spectra are

shown in Figure 3. Particular note should be taken of the phase spectrum, which is constant in the absorption region and random elsewhere. The absorption profiles were fit to gaussians by a nonlinear least squares method. Although the lineshapes are slightly pressure broadened and should be described by a Voigt profile, the signal-to-noise was not high enough to unambiguously fit that function.

In run sequence 2 the P(4.5) 1- line signal was measured as a function of flashing frequency. A 3.4 ma region near 3407.607 cm^{-1} was scanned at 1 x 10^{-5} A/s while I_o was recorded (5s time constant) simultaneously with the modulation components (4s time constant). This was done at four flashing frequencies, 7.8, 15.6, 31.3 and 62.5 Hz, performed in random order. To improve signal quality a series of measurements was made of the chemical modulation signal on a D.C. (unchopped) beam. Although these measurements give only relative amplitude information, since the IR detector does not respond to the D.C. beam amplitude, good phase shift measurements were produced.

Run sequence 3 investigated the intensities of the P(3.5) 2+ and P(3.5) 2- transitions relative the that of P(4.5) 1+. In the 3422.0 cm^{-1} region there are four H_2O lines suitable for frequency calibration. A fast scan over the spectral region containing these lines was performed using second derivative detection while the H_2O/O_3 mixture was being photolyzed. Figure 4 shows the four H_2O lines (A, D, E and F) clearly, as well as the peaks B and C which occur at frequencies corresponding to HO P(3.5) 2± lambda doublet lines. Next a set of scans over a 6.5 ma region overlapping peaks B and C was performed as before at a rate of 1 x 10^{-5} A/s. Immediately after these scans the laser and monochromator

were reset to the 3407.8 cm^{-1} region while keeping the chemical conditions constant and several fast scans made over the P(4.5) 1± lines. Although many sets of laser operating conditions were tried, a laser mode break persisted right at the P(4.5) 1- line frequency, so only the P(4.5) 1+ line was remeasured at a slow scanning rate. Since the ratio of the P(4.5) 1± lines had been measured previously, and the ratios of the P(3.5) 2± lines to the P(4.5) 1+ line were just measured, all line intensities could be related directly to that of the P(4.5) 1- transition.

HO Concentration Determination

HO radicals were produced in this photochemical system by the mechanism

$$O_3 + h\nu \ (2537 \text{ Å}) \rightarrow O_2 + O(^1D) \qquad (5)$$

$$O(^1D) + H_2O \rightarrow HO + HO \qquad (6)$$

Modulation of the photolysis rate induces periodic fluctuation of the HO concentration, which is the phenomenon being detected by the molecular modulation technique. Since the complete reaction mechanism describing this system is complex, time dependent numerical modeling was required to extract [HO] modulation amplitudes. A complete description of the 34 reaction mechanism and the rate constants used is given in Ref. 22. In addition to reaction rate constants, several other parameters are necessary to perform the calculations. Cell volume and gas flow rates were measured by standard expansion and water displacement techniques. Steady state [H_2O] under the standard flow conditions was measured by IR absorption[22] to be 6.8 x 10^{15} cm^{-3}. Steady state [O_3] was measured

by UV absorption at 315 nm both with and without photolysis occurring before every run sequence and after sequence 2. This allows calculation of O_3 flow-in rate and the D.C. photolysis flux. The ratio of the A.C. to D.C. photolysis rate was measured to be 0.65 using the UV photodiode which monitors the Hg lamps. With this information the [HO] modulation amplitude and phase relative to the photolysis lamps was calculated for the conditions measured before run 1 and both before and after run 2. These are listed in Table II, along with observed $[O_3]$. The uncertainty of the derived [HO] modulation amplitude on uncertainites in rate constants is discussed in the Appendix.

RESULTS AND DISCUSSION

The absolute intensity of the P(4.5) 1- transition was determined from analysis of runs 1 and 2. Peak absorption cross section σ_{peak} was calculated from the normalized modulation amplitude $(\Delta I/I_o)$ and calculated [OH] modulation amplitude Δn by the relation

$$(\Delta I/I_o)_{peak} = \sigma_{peak} \Delta n \ell \qquad (7)$$

where ℓ is the absorption pathlength. Run 1 gave a value $\sigma_{peak} = 2.21 \times 10^{-18}$ cm^2 molecule^{-1} and the 7.8 and 15.6 Hz data of Run 2 gave $\sigma_{peak} = 2.23 \pm 0.45 \times 10^{-18}$ cm^2 molecule^{-1} (1σ). The 31 and 63 Hz data of Run 2 were not included because of poor signal/noise. The linewidths obtained by fitting gaussian curves to the measured absorption profiles showed relatively large dispersion. This is attributed to laser frequency jitter and uneven current tuning, since all measurements were performed at the same temperature and pressure, and all four transitions are expected to have nearly equal linewidths. Therefore an average linewidth of 0.0138 ± 0.0016 cm^{-1} FWHM was calculated, weighting each measured

linewidth by the signal/noise of the measurement. This is 38% greater than the Doppler width at 300 K, and could be accounted for by pressure broadening by He, if a broadening coefficient of 0.11 cm^{-1} atm^{-1} FWHM is used. A separate determination of average linewidths for the P(4.5) 1± and P(3.5) 2± doublets indicated that they are equal to better than 1%. Since the peak absorption cross section, σ_{peak}, and the FWHM linewidth, W, were both obtained by fitting experimental profiles to gaussian curves, the integrated absorption coefficient (or line intensity) S is calculated by

$$S = (\pi/4\ \ell n\ 2)^{1/2}\ W\ \sigma_{peak} \qquad (8)$$

For the P(4.5) 1- transition, the line intensity is calculated to be $3.26 \pm 0.76 \times 10^{-20}$ cm^2 $molecule^{-1}$ cm^{-1}. Intensities for the other three transitions relative to P(4.5) 1- were calculated from the results of Runs 1 and 3. Where several scans were made of the same line, the results were averaged using the uncertainty from the fitting routine as a weighting function. The P(4.5) 1+ intensity was calculated from the P(4.5) 1+/P(4.5) 1- data of Run 1, and the P(3.5) 2± intensities from the Run 3 data, which measure these lines relative to P(4.5) 1+. The results are summarized in Table III. A comparison of observed and calculated HO phase shifts, Figure 5, shows good agreement, indicating that the measured HO chemical lifetime agrees with that predicted numerically, and confirms the validity of using calculated OH concentrations in this study.

The only other intensity information available on these HO transitions are the values calculated by Gillis and Goldman.[14] They obtain intensities

of 1.06×10^{-19} cm^2 $molecule^{-1}$ cm^{-1} and 5.95×10^{-20} cm^2 $molecule^{-1}$ cm^{-1}, respectively, for each of the doublet lines of the P(4.5) 1± and P(3.5) 2± line pairs, which are roughly three times larger than the values reported here. Since calculated intensities are usually good to a factor of two[23] and the experimental value have an uncertainty of 1.5 (2σ), the two studies are in rough agreement. Theory predicts that two lambda components of each vibration-rotation transition are nearly equal (± 0.3%), differing slightly due to a 0.8 cm^{-1} difference in lower state energy. The observed difference of about 13% for both the P(4.5) 1± and P(3.5) 2± doublets is probably just a reflection of the experimental uncertainty. The intensity ratio of P(3.5) 2±/P(4.5) 1± is predicted to be 0.561[14] and measured here as 0.572. Thus the results on relative intensities agree well with theory.

The results of this work are applicable in several areas. HO is a key reactive intermediate in many gas phase chemical systems, and with diode laser systems capable of measuring small (10^{-9} cm^{-1}) absorptions,[24] radical concentrations of 10^9 cm^{-3} should be detectable. This is not as sensitive as A → X resonance fluorescence detection, but circumvents the photochemical disruption which UV excitation can produce.[25] In the stratosphere HO concentrations have been measured in the 10^7 cm^{-3} range,[4] which may be detectable in the IR by exploiting the long path-lengths achieved by solar limb scanning techniques (1-50 $\times 10^5$ atm-cm), as has been done recently to measure the ClO radical.[26]

ACKNOWLEDGMENTS

This work was supported by the Director, Office of Energy Research, Office of Basic Energy Sciences, Chemical Sciences Division of the

U.S. Department of Energy under Contract Number DE-AC03-76SF00098. We wish to thank Dr. A. Goldman and Dr. J. G. Gillis for providing us with a listing of their HO line intensity results.

REFERENCES

1. M. W. Werner, S. Beckwith, J. Gatley, K. Sellgren, G. Berriman, and D. L. Whiting, Astrophys. J. 239, 540 (1980).

2. D. F. Dickinson, C. A. Gottlieb, E. W. Gottlieb, and M. M. Litvak, Astrophys. J. 206, 79 (1976).

3. P. A. Leighton, Photochemistry of Air Pollution (Academic Press, New York, 1961).

4. J. G. Anderson, Geophys. Res. Lett. 3, 165 (1976).

5. D. D. Drysdale and A. C. Lloyd, Oxidation Combustion Review (Elsevier, Amsterdam, 1970).

6. G. H. Dieke and H. M. Crosswhite, J. Quant. Spectrosc. Radiat. Transfer 2, 97 (1962).

7. J. L. Destombes, C. Marliere, and F. Rohart, J. Mol. Spectrosc. 67, 93 (1977).

8. I. L. Chidsey and D. R. Crosley, J. Quant. Spectrosc. Radiat. Transfer 23, 187 (1980).

9. A. Goldman and J. R. Gillis, J. Quant. Spectrosc. Radiat. Transfer 25, 111 (1981).

10. A. B. Meinel, Astrophys. J. 111, 555 (1950).

11. A. B. Meinel, Astrophys. J. 112, 120 (1950).

12. J. P. Maillard, J. Chauville, and A. W. Mantz, J. Mol. Spectrosc. 63, 120 (1976).

13. J. A. Coxon, Can. J. Phys. 58, 933 (1980).

14. J. R. Gillis and A. Goldman, J. Quant. Spectrosc. Radiat. Transfer 26, 23 (1981).

15. F. Roux J. D'Incan, and D. Cerny, Astrophys. J. 186, 1141 (1973).

16. J. U. White, J. Opt. Soc. Am. 32, 285 (1942).

17. J. Reid, J. Shewchun, B. K. Garside, and E. A. Ballick, Appl. Opt. 17, 300 (1978).

18. E. D. Hinkley, Laser Monitoring of the Atmosphere (Springer-Verlag, New York, 1976).

19. H. S. Johnston, G. E. McGraw, T. T. Paukert, L. W. Richards, and J. Van den Bogaerde, Proc. Natl. Acad. Sci. 57, 1146 (1967).

20. J. M. Brown, J. T. Hougen, K.-P. Huber, J. W. C. Johns, I. Kopp, H. Lefebvre-Brian, A. J. Merer, D. A. Ramsay, J. Rostas, and R. N. Zare, J. Mol. Spectrosc. 55, 500 (1975).

21. J. M. Flaud and C. Camy-Peyret, J. Mol. Spectrosc. 55, 278 (1975).

22. J. Podolske and H. S. Johnston, J. Phys. Chem. 87, 628 (1983).

23. A. Komornicki and R. L. Jaffe, J. Chem. Phys. 71, 2150 (1979).

24. J. Reid, M. El-Sherbiny, B. K. Garside, and E. A. Ballick, Appl. Opt. 19, 3349 (1980).

25. D. D. Davis, M. O. Rodgers, S. D. Fischer, and K. Asai, Geophys. Res. Lett. 8, 69 (1981).

26. R. T. Menzies, Geophys. Res. Lett. 6, 151 (1979).

27. World Meteorological Organization, The Stratosphere 1981 Theory and Measurements. Editor, Robert Hudson. Code 963, NASA/Goddard Space Flight Center, Greenbelt, Maryland 20771.

Table I. Observed transitions of HO and H_2O.

Species	ν (cm^{-1})	Designation	Reference
HO	3407.607	P(4.5) 1-	12
H_2O	3407.826		21
HO	3407.989	P(4.5) 1+	12
H_2O	3421.739		21
HO	3421.936	P(3.5) 2-	12
HO	3422.012	P(3.5) 2+	12
H_2O	3422.272		21
H_2O	3422.333		21
H_2O	3422.369		21

Table II. Measured O_3 and calculated OH modulation behavior.

Run	O_3 (dark) (10^{15} molecules/cm^3)	$O_3(H_2O + h\nu)$ (10^{15} molecules/cm^3)	Mod. Freq. (Hz)	Calculated Phase (deg)	[OH] Modulation Amplitude (10^{11} molecules/cm^3)
pre-1	17.18	2.053	15.625	-19.22 ± 0.53	4.56 ± 0.34
pre-2	17.14	2.056	-	-	-
<2>[a]			7.8125	- 9.53 ± 0.75	3.95 ± 0.89
<2>[a]			15.625	-18.32 ± 1.17	3.82 ± 0.85
<2>[a]			31.25	-34.43 ± 1.90	3.35 ± 0.69
<2>[a]			62.5	-54.47 ± 1.85	2.36 ± 0.44
post-2	14.15	2.400	-	-	-
pre-3	18.62	2.334	-	-	-

[a]Listed phase and amplitude are average of results calculated using pre-2 and post-2 conditions.

Table III. HO line intensity results.

Line	Run	Modulation Ampl. ($\Delta I/I_o$)	Intensity (cm^2 $molecule^{-1}$ cm^{-1})
P(4.5) 1-	1	$2.98 \pm 0.26 \times 10^{-3}$	$3.26 \pm 1.52 \times 10^{-20}$
P(4.5) 1+	1	$2.62 \pm 0.74 \times 10^{-3}$	$2.87 \pm 1.58 \times 10^{-20}$
P(4.5) 1+	3	$1.82 \pm 0.42 \times 10^{-3}$	$2.87 \pm 1.58 \times 10^{-20}$
P(4.5) 2-	3	$1.04 \pm 0.48 \times 10^{-3}$	$1.64 \pm 1.22 \times 10^{-20}$
P(4.5) 2+	3	$1.18 \pm 0.38 \times 10^{-3}$	$1.85 \pm 1.32 \times 10^{-20}$

Listed uncertainties are two standard deviations.

FIGURE CAPTIONS

Figure 1. Energy level diagram for the HO molecules. The transitions observed in this study are indicated, with the notation following Ref. 12. The number and sign at the end indicate spin orbit state (F_1 or F_2) and parity, respectively, of the lower state. e/f labeling of each state is also shown (Ref. 20).

Figure 2. Diode laser scan in 3407.8 cm^{-1} region. Upper trace is a first derivative spectrum of unphotolyzed H_2O/O_3 mixture; peak C corresponds to the 3407.826 cm^{-1} H_2O line. Middle trace is the fringe pattern of Ge etalon (0.0486 cm^{-1} free spectral range). Lower trace is modulation signal amplitude during modulated photolysis of H_2O/O_3; peaks A and B correspond to HO lambda doublet lines at 3407.607 cm^{-1} and 3407.989 cm^{-1}, respectively.

Figure 3. Modulation phase and amplitude spectrum for the P(4.5) 1- HO transition at 3407.607 cm^{-1}.

Figure 4. Diode laser scan in 3422.0 cm^{-1} region. Upper trace is a second derivative scan of a photolyzed H_2O/O_3 mixture; peaks B and C correspond to the HO P(3.5) 2± lambda doublet lines at 3421.936 cm^{-1} and 3422.012 cm^{-1}, peaks A, D, E, and F correspond to H_2O lines at 3421.739, 3422.272, 3422.333, and 3422.369 cm^{-1}. Middle trace shows direct absorption

signal; lines A, E and F are discernible. Lower trace is of Ge etalon (0.0486 cm^{-1} fringe spacing).

Figure 5. Calculated and experimental HO phase shift versus photolytic flashing frequency.

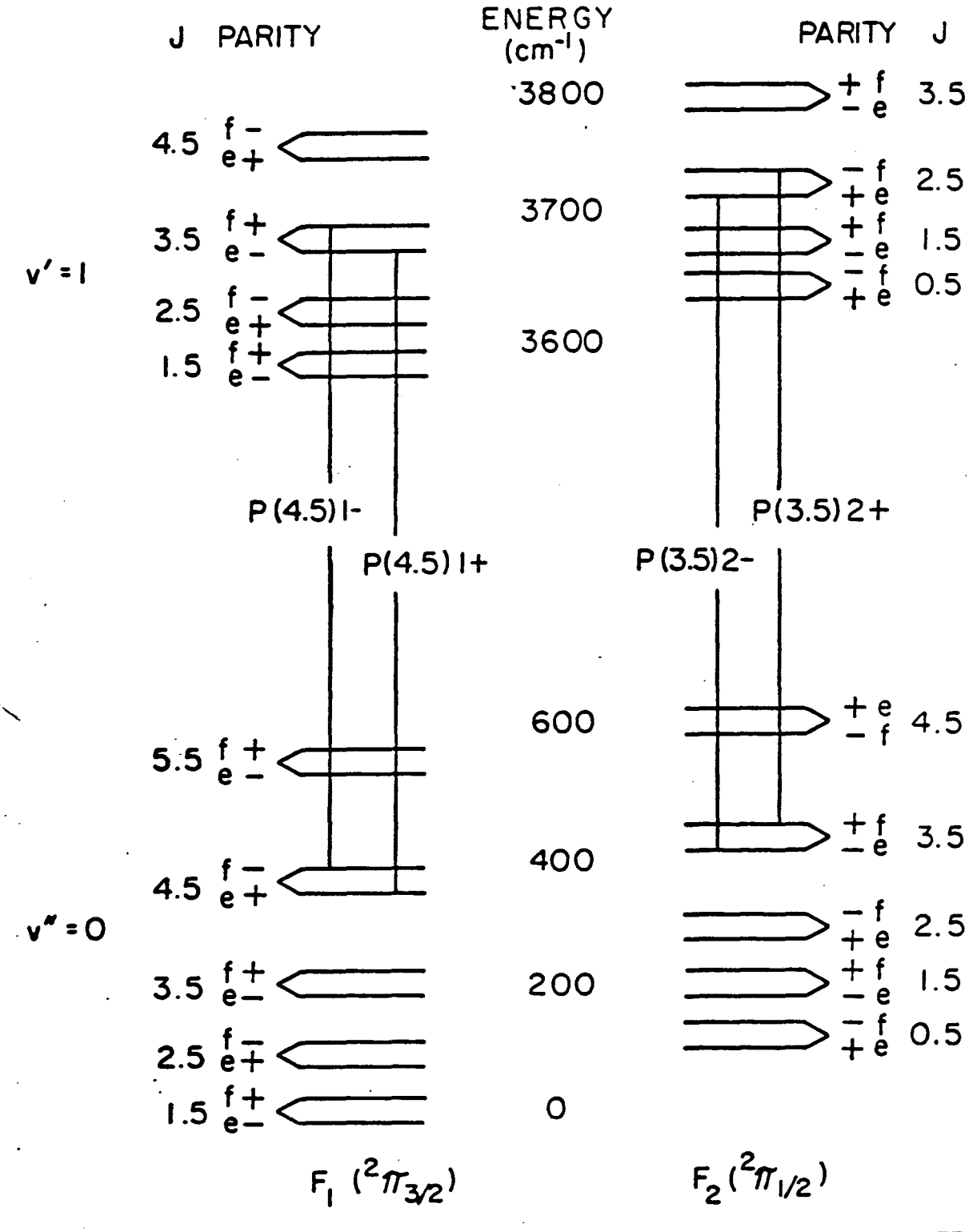
J PARITY
ENERGY (cm⁻¹)
PARITY J
3800
3700
3600
600
400
200
0
v' = 1
v'' = 0
4.5 f − e +
3.5 f + e −
2.5 f − e +
1.5 f + e −
5.5 f + e −
4.5 f − e +
3.5 f + e −
2.5 f − e +
1.5 f + e −
+ f − e 3.5
− f + e 2.5
+ f − e 1.5
− f + e 0.5
+ e − f 4.5
+ f − e 3.5
− f + e 2.5
+ f − e 1.5
− f + e 0.5
P(4.5) 1−
P(4.5) 1+
P(3.5) 2+
P(3.5) 2−
F1 (2π3/2)
F2 (2π1/2)

XBL 818-6377

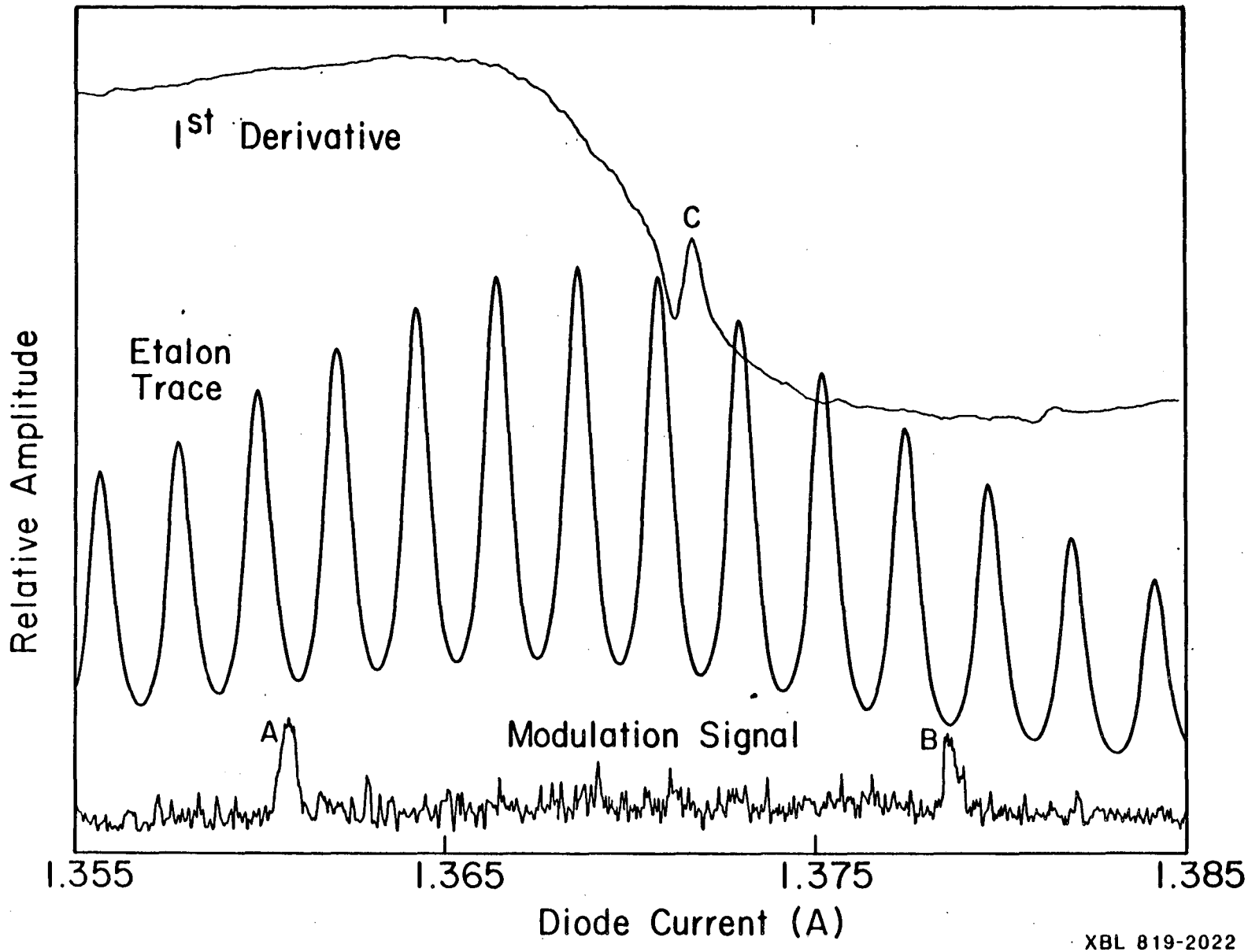
1st Derivative
C
Etalon
Trace
Relative Amplitude
A
Modulation Signal
B
1.355
1.365
1.375
1.385
Diode Current (A)

XBL 819-2022

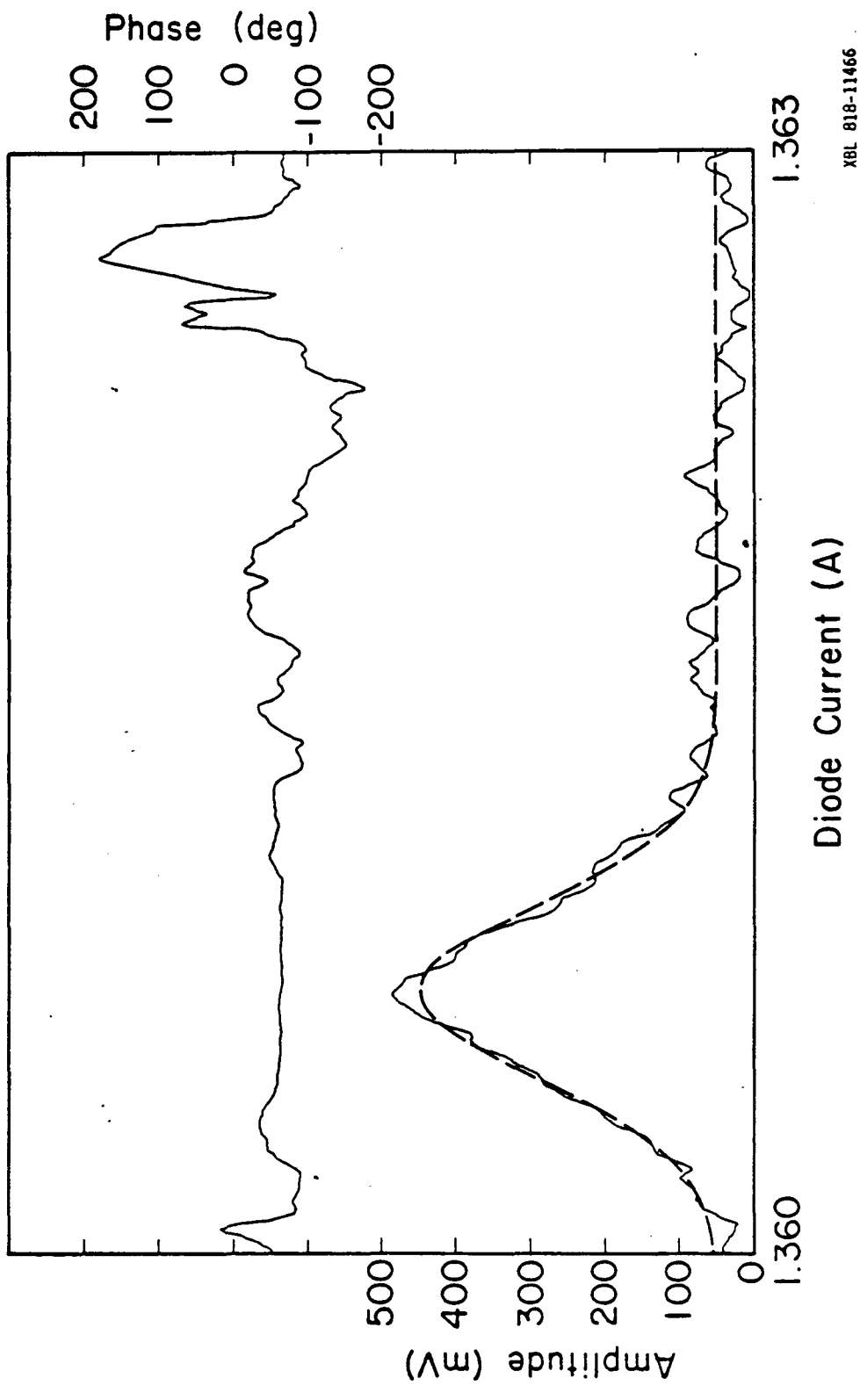
Phase (deg)
200
100
0
-100
-200
1.363
1.360
Diode Current (A)
Amplitude (mV)
500
400
300
200
100
0
XBL 818-11466

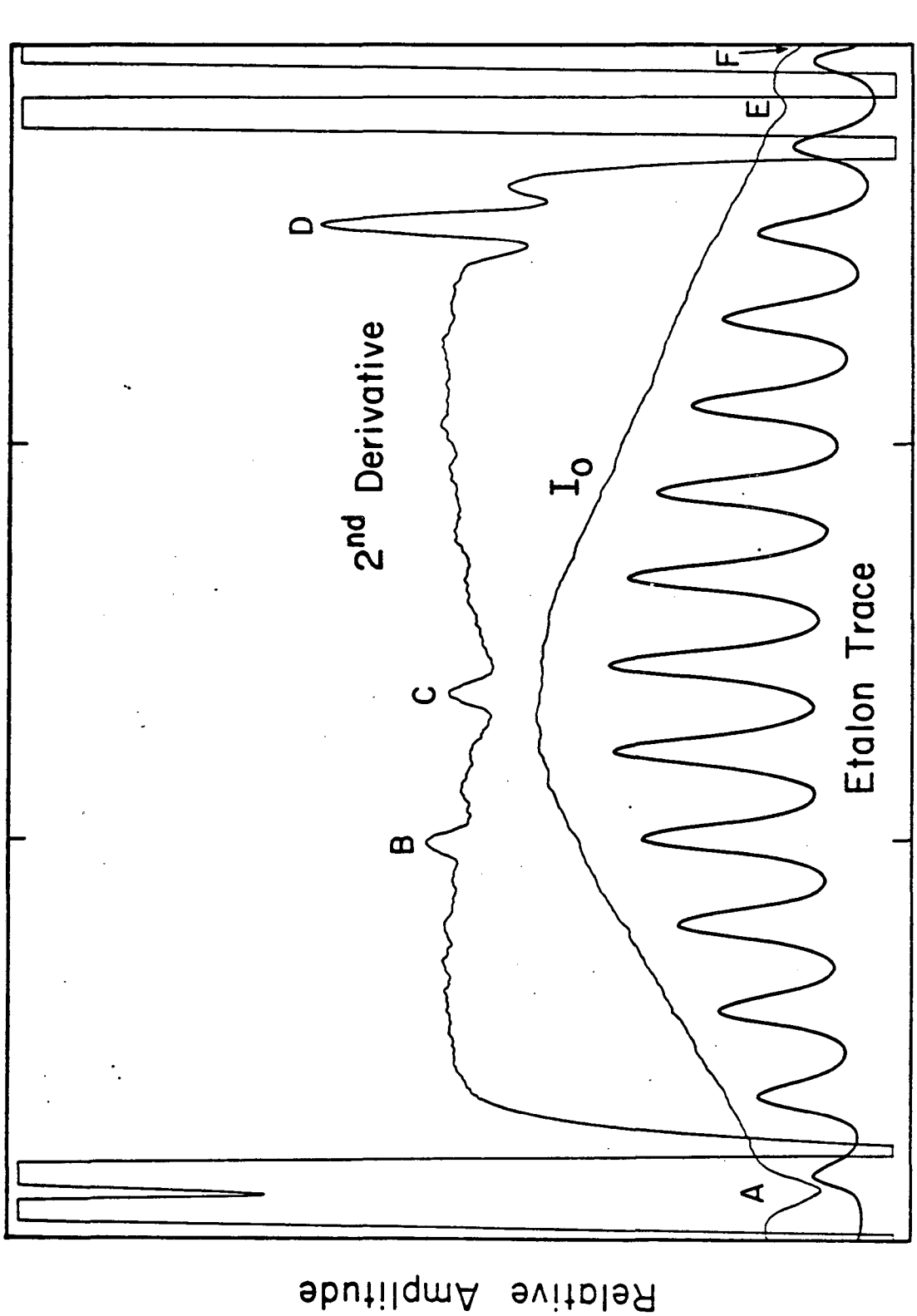

XBL 818-11460

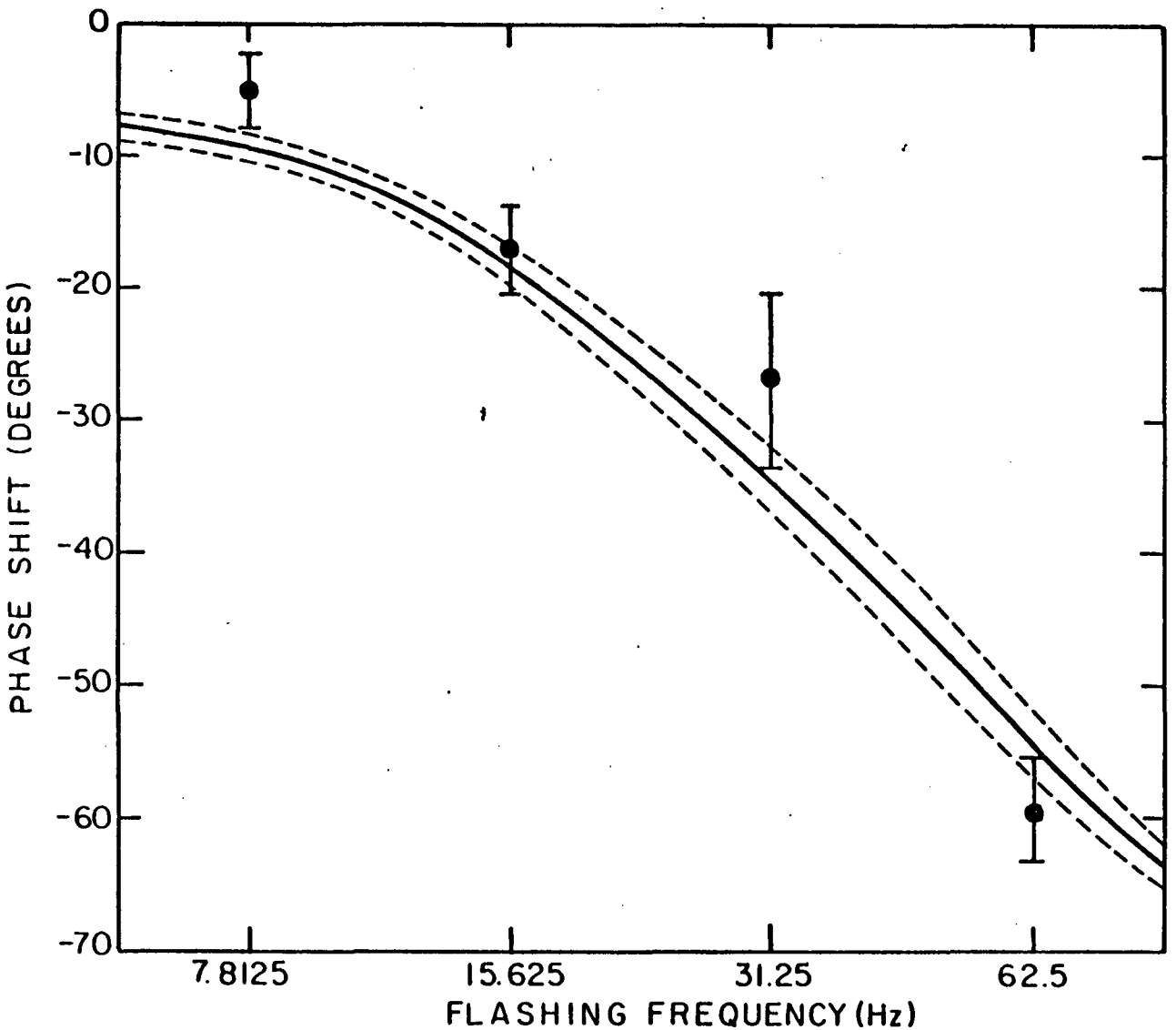
0
-10
-20
-30
-40
-50
-60
-70
PHASE SHIFT (DEGREES)
7.8125
15.625
31.25
62.5
FLASHING FREQUENCY (Hz)

XBL 818-6373

APPENDIX — SYSTEMATIC ERRORS

An obvious source of systematic error in this procedure is uncertainty in the rate constants used to calculate the concentration of hydroxyl radicals. However, in this experiment the results are dominated by only four reactions, mechanism I.

1. $O_3 + h\nu \rightarrow O_2 + O(^1D)$
5. $O(^1D) + H_2O \rightarrow 2HO$
21. $HO + O_3 \rightarrow HOO + O_2$
24. $HO + HOO \rightarrow H_2O + O_2$

where equation numbers are those of Ref. 22.

For this mechanism the steady-state concentration of hydroxyl radicals is

$$[HO] = j_1/k_{21} \tag{A1}$$

which is independent of the values of k_5 and k_{24}, even though these reactions occur in the mechanism. The mechanism can be improved if one calculates the fraction α of $O(^1D)$ that reacts with water

$$\alpha = k_5[H_2O]/\Sigma k_m[M] \tag{A2}$$

where M are H_2O, O_3 (two channels), O_2, and He. In these experiments α is about 0.9 and is weakly dependent on the four additional rate coefficients used in its evaluation. Mechanism II includes these four rate coefficients plus the four of mechanism I and yields the expression:

$$[HO] = \alpha j_1/k_{21} \tag{A3}$$

Although the chain length for ozone destruction by HO_x is very short under conditions of these experiments, it is interesting to add the second chain step

$$26. \qquad HOO + O_3 \rightarrow HO + O_2 + O_2$$

to give mechanism III, which yields the relation

$$2[HO] = R + (R^2 + 4Rk_{26}[O_3]/k_{24})^{1/2} \qquad (A4)$$

where R is $\alpha j_1/k_{21}$.

Finally, mechanism IV is the set of 32 reactions that includes a 10% contribution of

$$2. \qquad O_3 + h\nu \rightarrow O_2 + O(^3P)$$

and subsequent reactions of atomic oxygen. Also included are the formation and reactions of H_2O_2, $O_2(^1\Delta)$, and atomic hydrogen.

The calculated modulation amplitude of the hydroxyl radicals (that for $I + \Delta I$ minus that for $I - \Delta I$ for slow oscillations of the light intensity) is given in Table IV for each of the four mechanisms, involving a typical set of experimental conditions. For the simple four-step mechanism I the calculated concentration of hydroxyl radicals depends only on j_1 and k_{21}, (A1); the coefficient j_1 was measured in this apparatus; and the coefficient k_{21} is regarded to be uncertain[27] to a factor of 1.25. In units of 10^{11} molecules cm^{-3}, the concentration of hydroxyl radicals is 6.4 according to mechanism I; it is reduced to 5.9 by considering the relatively error free factor α (A2); mechanism III gives 5.7; and the full 32 reaction mechanism IV gives 5.1. The important part of this discussion is that the full 32 step mechanism

provides merely a 20% correction to the four-step mechanism I (A1) and only an 11% correction to the nine-step mechanism III (A4). The expected systematic error due to uncertainties in rate coefficients depends primarily on two values, j_1 and k_{21} (Eq. A1); and it depends weakly on uncertainties in the other 30 reactions. In this study we ascribe ± 25% uncertainty to this source of systematic error.

Table IV. Comparison of calculated modulation amplitude for hydroxyl radicals for four mechanisms of difference complexity (based on one typical experiment).

Mechanism	Number of reactions	Eq. No.	Calculated modulation amplitude of HO/10^{11}
I	4	A1	6.4
II	8	A3	5.9
III	9	A4	5.7
IV	32	-	5.1

Concentrations at steady state: O_3, 2.1 x 10^{15}; O_2, 2.4 x 10^{16}; H_2O, 6.9 x 10^{16}; He, 2.2 x 10^{18} molecules cm^{-3}. Light intensity: DC, 6.7 x 10^{15}; modulation amplitude, 4.3 x 10^{15} photons cm^{-2} s^{-1}. Value of α (Eq. A2): 0.92.

This report was done with support from the Department of Energy. Any conclusions or opinions expressed in this report represent solely those of the author(s) and not necessarily those of The Regents of the University of California, the Lawrence Berkeley Laboratory or the Department of Energy.

Reference to a company or product name does not imply approval or recommendation of the product by the University of California or the U.S. Department of Energy to the exclusion of others that may be suitable.

TECHNICAL INFORMATION DEPARTMENT
LAWRENCE BERKELEY LABORATORY
UNIVERSITY OF CALIFORNIA
BERKELEY, CALIFORNIA 94720